Decoupled front/back dielectric textures for flat ultra-thin c-Si solar cells

Isabella, Olindo; Vismara, Robin; Ingenito, Andrea; Rezaei, Nasim; Zeman, M.

DOI
10.1364/OE.24.00A708

Publication date
2016

Document Version
Final published version

Published in
Optics Express

Decoupled front/back dielectric textures for flat ultra-thin c-Si solar cells

Olindo Isabella,* Robin Vismara, Andrea Ingenito, Nasim Rezaei, and M. Zeman

Delft University of Technology, Photovoltaic Material and Devices, Mekelweg 4, 2628CD Delft, The Netherlands
o.isabella@tudelft.nl

Abstract: The optical analysis of optically-textured and electrically-flat ultra-thin crystalline silicon (c-Si) slabs is presented. These slabs were endowed with decoupled front titanium-dioxide (TiO_2) / back silicon-dioxide (SiO_2) dielectric textures and were studied as function of two types of back reflectors: standard silver (Ag) and dielectric modulated distributed Bragg reflector (MDBR). The optical performance of such systems was compared to that of state-of-the-art flat c-Si slabs endowed with so-called front *Mie resonators* and to those of similar optical systems still endowed with the same back reflectors and decoupled front/back texturing but based on textured c-Si and dielectric coatings (front TiO_2 and back SiO_2). Our optimized front dielectric textured design on 2-μm thick flat c-Si slab with MDBR resulted in more photo-generated current density in c-Si with respect to the same optical system but featuring state-of-the-art Mie resonators (+ 6.4%), mainly due to an improved light in-coupling between 400 and 700 nm and light scattering between 700 and 1050 nm. On the other hand, the adoption of textured dielectric layers resulted in less photo-generated current density in c-Si up to −20.6% with respect to textured c-Si, depending on the type of back reflector taken into account.

OCIS codes: (050.0050) Diffraction and gratings; (040.6040) Silicon.

References and links

1. I. S. E. Fraunhofer, "Photovoltaics report" (Fraunhofer ISE 2015). *https://www.ise.fraunhofer.de/de/downloads/pdf-files/aktuelles/photovoltaics-report-in-englischer-sprache.pdf*
2. ITRPV, "International Technology Roadmap for Photovoltaic, 6th edition" (ITRPV, 2015). *http://www.itrpv.net/Reports/Downloads/2015/*
3. S. B. Mallick, M. Agrawal, and P. Peumans, "Optimal light trapping in ultra-thin photonic crystal crystalline silicon solar cells," Opt. Express **18**(6), 5691–5706 (2010).
4. Y. Park, E. Drouard, O. El Daif, X. Letartre, P. Viktorovitch, A. Fave, A. Kaminski, M. Lemiti, and C. Seassal, "Absorption enhancement using photonic crystals for silicon thin film solar cells," Opt. Express **17**(16), 14312–14321 (2009).
5. J. Li, H. Y. Yu, S. M. Wong, G. Zhang, G.-Q. Lo, and D.-L. Kwong, "Si nanocone array optimization on crystalline Si thin films for solar energy harvesting," J. Phys. D Appl. Phys. **43**(25), 255101 (2010).
6. S. E. Han and G. Chen, "Toward the Lambertian limit of light trapping in thin nanostructured silicon solar cells," Nano Lett. **10**(11), 4692–4696 (2010).
7. M. D. Kelzenberg, S. W. Boettcher, J. A. Petykiewicz, D. B. Turner-Evans, M. C. Putnam, E. L. Warren, J. M. Spurgeon, R. M. Briggs, N. S. Lewis, and H. A. Atwater, "Enhanced absorption and carrier collection in Si wire arrays for photovoltaic applications," Nat. Mater. **9**(3), 239–244 (2010).
8. W. Wang, S. Wu, K. Reinhardt, Y. Lu, and S. Chen, "Broadband light absorption enhancement in thin-film silicon solar cells," Nano Lett. **10**(6), 2012–2018 (2010).
9. J. Grandidier, D. M. Callahan, J. N. Munday, and H. A. Atwater, "Light absorption enhancement in thin-film solar cells using whispering gallery modes in dielectric nanospheres," Adv. Mater. **23**(10), 1272–1276 (2011).
10. J. Bhattacharya, N. Chakravarty, S. Pattnaik, W. Dennis Slafer, R. Biswas, and V. L. Dalal, "A photonic-plasmonic structure for enhancing light absorption in thin film solar cells," Appl. Phys. Lett. **99**(13), 131114 (2011).
11. U. W. Paetzold, E. Moulin, D. Michaelis, W. Bottler, C. Wachter, V. Hagemann, M. Meier, R. Carius, and U. Rau, "Plasmonic reflection grating back contacts for microcrystalline silicon solar cells," Appl. Phys. Lett. **99**(18), 181105 (2011).
12. R. Dewan, I. Vasilev, V. Jovanov, and D. Knipp, "Optical enhancement and losses of pyramid textured thin-film silicon solar cells," J. Appl. Phys. **110**(1), 013101 (2011).

#257616 Received 18 Jan 2016; revised 26 Feb 2016; accepted 29 Feb 2016; published 17 Mar 2016

13. X. Sheng, S. G. Johnson, J. Michel, and L. C. Kimerling, "Optimization-based design of surface textures for thin-film Si solar cells," Opt. Express **19**(S4), A841–A850 (2011).
14. J. Gjessing, A. S. Sudbo, and E. S. Marstein, "Comparison of periodic light-trapping structures in thin crystaline silicon solar cells," J. Appl. Phys. **110**(3), 033104 (2011).
15. R. Biswas and C. Xu, "Nano-crystalline silicon solar cell architecture with absorption at the classical $4n(^2)$ limit," Opt. Express **19**(S4), A664–A672 (2011).
16. S. Fahr, T. Kirchartz, C. Rockstuhl, and F. Lederer, "Approaching the Lambertian limit in randomly textured thin-film solar cells," Opt. Express **19**(S4), A865–A874 (2011).
17. R. Y. Zhang, B. Shao, J. R. Dong, J. C. Zhang, and H. Yang, "Absorption enhancement analysis of crystalline si thin film solar cells based on broadband antireflection nanocone grating," J. Appl. Phys. **110**(11), 113105 (2011).
18. K. X. Wang, Z. Yu, V. Liu, Y. Cui, and S. Fan, "Absorption enhancement in ultrathin crystalline silicon solar cells with antireflection and light-trapping nanocone gratings," Nano Lett. **12**(3), 1616–1619 (2012).
19. O. Isabella, A. Ingenito, D. Linssen, and M. Zeman, "Front/rear decoupled texturing in refractive and diffractive regimes for ultra-thin silicon-based solar cells," *OSA Technical Digest (online)* (Optical Society of America, 2013), paper PM4C.2.
20. A. Ingenito, O. Isabella, and M. Zeman, "Experimental Demonstration of $4n^2$ Classical Absorption Limit in Nanotextured Ultrathin Solar Cells with Dielectric Omnidirectional Back Reflector," ACS Photonics **1**(3), 270–278 (2014).
21. T. Tiedje, E. Yablonovitch, G. D. Cody, and B. G. Brooks, "Limiting Efficiency of Silicon Solar Cells," IEEE Trans. Electron Dev. **31**(5), 711–716 (1984).
22. S. Fan, W. Suh, and J. D. Joannopoulos, "Temporal coupled-mode theory for the Fano resonance in optical resonators," J. Opt. Soc. Am. A **20**(3), 569–572 (2003).
23. Z. Yu, A. Raman, and S. Fan, "Fundamental limit of light trapping in grating structures," Opt. Express **18**(S3), A366–A380 (2010).
24. A. H. M. Smets, K. Jäger, O. Isabella, R. A. C. M. M. van Swaaij, and M. Zeman, *Solar Energy – The Physics and Engineering of Photovoltaic Conversion, Technologies and Systems* (UIT Cambridge, 2016).
25. A. Ingenito, O. Isabella, and M. Zeman, "Nano-cones on micro-pyramids: modulated surface textures for maximal spectral response and high-efficiency solar cells," Prog. Photovolt. Res. Appl. **23**(11), 1649–1659 (2015).
26. P. Spinelli, M. A. Verschuuren, and A. Polman, "Broadband omnidirectional antireflection coating based on subwavelength surface Mie resonators," Nat. Commun. **3**, 692 (2012).
27. J. Krč, M. Zeman, S. L. Luxembourg, and M. Topic, "Modulated photonic-crystal structures as broadband back reflectors in thin-film solar cells," Appl. Phys. Lett. **94**(15), 153501 (2009).
28. ANSYS white papers (ANSYS 2015). *http://www.ansys.com/Products/Electronics/ANSYS-HFSS*
29. O. Isabella, S. Solntsev, D. Caratelli, and M. Zeman, "3-D optical modeling of thin-film silicon solar cells on diffraction gratings," Prog. Photovolt. Res. Appl. **21**(1), 94–108 (2013).
30. M. Zeman, O. Isabella, S. Solntsev, and K. Jäger, "Modelling of thin-film silicon solar cells," Sol. Energy Mater. Sol. Cells **119**, 94–111 (2013).
31. O. Isabella, H. Sai, M. Kondo, and M. Zeman, "Full-wave optoelectrical modeling of optimized flattened light-scattering substrate for high efficiency thin-film silicon solar cells," Prog. Photovolt. Res. Appl. **22**(6), 671–689 (2014).
32. NREL, "Reference solar spectral irradiance: Air Mass 1.5" (NREL, 2015). *http://rredc.nrel.gov/solar/spectra/am1.5/*
33. W. Shockley and H. J. Queisser, "Detailed balance limit of efficiency of pn junction solar cells," J. Appl. Phys. **32**(3), 510 (1961).
34. A. Ingenito, S. L. Luxembourg, P. Spinelli, J. Liu, J. C. Ortiz Lizcano, A. W. Weeber, O. Isabella, and M. Zeman, "Optimized metal-free back reflectors for high efficiency open rear c-Si solar cells," IEEE J. Photovolt. **6**(1), 34–40 (2016).
35. Z. C. Holman, S. De Wolf, and C. Ballif, "Improving metal reflectors by suppressing surface plasmon polaritons: *a priori* calculation of the internal reflectance of a solar cell," Light Sci. Appl. **2**(10), e106 (2013).
36. P. Kowalczewski and L. C. Andreani, "Towards the efficiency limits of silicon solar cells: How thin is too thin?" Sol. Energy Mater. Sol. Cells **143**, 260–268 (2015).
37. C. S. Schuster, A. Bozzola, L. C. Andreani, and T. F. Krauss, "How to assess light trapping structures versus a Lambertian Scatterer for solar cells?" Opt. Express **22**(S2), A542–A551 (2014).
38. S. L. Luxembourg, P. Spinelli, A. Ingenito, J. Liu, O. Isabella, M. Zeman, and A. W. Weeber, "A benchmarking study of the application of a distributed Bragg reflector as back-reflector on n-Pasha solar cells," 31st European Photovoltaic Solar Energy Conference and Exhibition, 972–975 (2015).
39. O. Isabella, S. Solntsev, D. Caratelli, and M. Zeman, "3-D optical modeling of single and multi-junction thin-film silicon solar cells on gratings," MRS Proc. **1426**, 149–154 (2012).
40. B. Lipovšek, M. Cvek, A. Čampa, J. Krč, and M. Topič, "Analysis and Optimisation of Periodic Interface Textures in Thin-Film Silicon Solar Cells," in 25th European Photovoltaic Solar Energy Conference and Exhibition (2010), pp. 3120–3123.
41. S. Solntsev, O. Isabella, D. Caratelli, and M. Zeman, "Thin-film silicon solar cells on 1-D periodic gratings with nonconformal layers: optical analysis," IEEE J. Photovolt. **3**(1), 46–52 (2013).
42. C. Ducros and H. Szambolics, "Method for producing a textured reflector for a thin-film photovoltaic cell, and resulting textured reflector," *https://www.google.com/patents/WO2013160570A1*.

#257616 Received 18 Jan 2016; revised 26 Feb 2016; accepted 29 Feb 2016; published 17 Mar 2016

43. H. Sai and M. Kondo, "Effect of self-orderly textured back reflectors on light trapping in thin-film microcrystalline silicon solar cells," Appl. Phys. Lett. **105**, 094511 (2009).
44. H. Sai, H. Fujii, K. Arafune, Y. Ohshita, Y. Kanamori, H. Yugami, and M. Yamaguchi, "Wide-angle antireflection effect of subwavelength structures for solar cells," Jpn. J. Appl. Phys. **46**(6A), 3333–3336 (2007).
45. K. Söderström, G. Bugnon, R. Biron, C. Pahud, F. Meillaud, F.-J. Haug, and C. Ballif, "Thin-film silicon triple-junction solar cell with 12.5% stable efficiency on innovative flat light-scattering substrate," J. Appl. Phys. **112**(11), 114503 (2012).
46. A. Naqavi, F.-J. Haug, K. Söderström, C. Battaglia, V. Paeder, T. Scharf, H. P. Herzig, and C. Ballif, "Angular behavior of the absorption limit in thin film silicon solar cells," Prog. Photovolt. Res. Appl. **22**(11), 1147–1158 (2014).
47. R. Santbergen, H. Tan, M. Zeman, and A. H. M. Smets, "Enhancing the driving field for plasmonic nanoparticles in thin-film solar cells," Opt. Express **22**(S4), A1023–A1028 (2014).
48. H. Savin, P. Repo, G. von Gastrow, P. Ortega, E. Calle, M. Garín, and R. Alcubilla, "Black silicon solar cells with interdigitated back-contacts achieve 22.1% efficiency," Nat. Nanotechnol. **10**(7), 624–628 (2015).
49. L. Wang, A. Lochtefeld, J. Han, A. P. Gerger, M. Carroll, J. Ji, A. Lennon, H. Li, R. Opila, and A. Barnett, "Development of a 16.8% efficient 18-μm silicon solar cell on steel," IEEE J. Photovolt. **4**(6), 1397–1404 (2016).

1. Introduction

Crystalline silicon (c-Si) currently dominates the photovoltaic (PV) market [1]. Light trapping is of utmost importance to meet the roadmap of c-Si PV, which is pointing towards wafers' thinning and targeting 60-μm thick wafers by 2020 [2]. Going beyond such target, ultra-thin (nano-/micro-/multi-)c-Si solar cells have attracted a lot of attention in last the few years [3–18]. These devices are characterized by thin c-Si absorber layers (< 20 μm), which minimize material consumption and potentially manufacturing costs. However, the reduced thickness results in a decrease of light absorption, i.e. lower photo-generated current density (J_{ph}).

To oppose this behavior, especially at long wavelengths close to the wavelength equivalent to the band gap of c-Si, light-management techniques should be implemented. Recently, it has been shown both theoretically [18,19] and experimentally [20] that decoupled front/back textured Si exhibits absorption enhancement over a broad wavelength range, i.e. between 300 nm and 1200 nm, with respect to a flat Si slab. In particular, for few microns thick c-Si slabs paired with an optimized back reflector (BR), the maximal absorption of light [21] can be reached [20]. On the other hand, according to the temporal mode couple theory [22], this maximal absorption - known as the *$4n^2$ limit* - where n is the real part of the refractive index of the absorbing dielectric slab, might be even surpassed in relatively narrow spectral ranges for micron and sub-micron thick Si slabs endowed with periodic gratings [23].

With the decoupled texturing approach it is possible to achieve a broad-band anti-reflective effect depending on the aspect ratio of the surface features. These structures, consisting of textures with different geometrical dimensions between slab's front and back side, allow to maximize (i) light in-coupling (via front nano-texturing) and (ii) long-wavelength scattering (via back micro-texturing). The first aspect means a reflectance (R) well below 1% between 300 nm and 800-1000 nm (depending on slab's thickness) due to a smooth refractive index transition from air to silicon. The second aspect means that the Si absortance (A_{Si}) approaches or even surpasses the $4n^2$ limit between 800 and 1000 nm and 1200 nm due to the coupling of light into wave guided modes available within the Si slab. However, texturing Si increases the loss mechanism known as surface recombination, resulting in lower open-circuit voltage (V_{OC}) and fill-factor (FF) with respect to an equivalent flat device [24]. As a consequence, surface passivation and texturing methods resulting in few surface defects are instrumental to reach high conversion efficiencies [25].

Recently, into an attempt to keep high both V_{OC} and J_{ph}, a novel flat c-Si solar cell architecture has been proposed [26] endowed with a front passivating textured dielectric, whose features are known as *Mie resonators*. Such architecture presents an intriguing dichotomy between *optically-textured* and *electrically-flat* interfaces. In this contribution we optically investigate such dichotomy applied to a 2-μm thick flat c-Si slab. In particular, we study the optical effect that two different types of back reflector have on A_{Si} posed just after the rear silicon-dioxide (SiO_2): a standard silver (Ag) layer and a dielectric Modulated Distributed Bragg Reflector (MDBR) [27]. The light absorption enhancement of the proposed

#257616 Received 18 Jan 2016; revised 26 Feb 2016; accepted 29 Feb 2016; published 17 Mar 2016

flat c-Si combined with decoupled front/back dielectric textures based on titanium-dioxide (TiO_2) at the front and SiO_2 at the back is compared to the equivalent structures based on textured c-Si and merely coated with TiO_2 at the front and SiO_2 / reflector at the back.

2. Modelling approach

The performance of different optical systems shown in this work was analyzed by means of three-dimensional (3-D) optical modelling. The Ansoft® High Frequency Structure Simulator software (HFSS) [28] was employed. This is a Maxwell equations solver based on the finite element method that allows for the optical design and simulation of opto-electrical devices with arbitrarily complex 3-D structures [29–31], that we call *models*. The different models were optically evaluated determining R and transmittance (T) of the optical system and the absorptance in each layer (A_i, where i indicates the i-th material comprised in the model). R and T were calculated in terms of S-parameters [28,29]. A_i was computed as the integral, over the layer volume V_i, of the square of the magnitude of the electric field E:

$$A_i(\lambda) = \frac{1}{2}\varepsilon_0 \,\mathrm{Im}(\varepsilon_i)\omega \int_{V_i} |E|^2 \, dV \tag{1}$$

where λ is the wavelength of light *in vacuo*, ε_0 is the dielectric constant of vacuum, ε_i is the (complex) relative permittivity of the i-th material, and ω is the angular frequency of the incident wave. The implied photo-generated current density ($J_{\text{ph-}i}$) in c-Si, lost in supporting layers and related to R and/or T could be determined by convoluting the absorptance A_i or R and T with the reference AM1.5 spectral photon flux $\Phi(\lambda)$ [32] within the relevant wavelength range (300-1200 nm):

$$J_{ph-i}(\lambda) = -q \int_{300\,nm}^{1200\,nm} A_i(\lambda)\Phi(\lambda)d\lambda \text{ and } J_{ph-R\text{ or }T}(\lambda) = -q \int_{300\,nm}^{1200\,nm} R(\lambda)\text{ or }T(\lambda)\Phi(\lambda)d\lambda \tag{2}$$

where q represents the elementary charge. Further details on the modelling process can be found in references [29–31]. At any simulated wavelength of each model, the sum of all contributions (reflectance, absorptances and eventual transmittance) was equal to one, ensuring the energy conservation of our modelling approach. In this respect, setting $\Phi(\lambda)$ as the only integrand in Eq. (2) (i.e. $1 \cdot \Phi(\lambda)$ for any λ) yields 46.19 mA/cm^2. This value is the Shockley-Queisser limit of photo-current density, which is, given a spectral photon flux such as the AM1.5, the maximal available implied phot-current density in a certain wavelength range [33] (in our work between 300 nm and 1200 nm). The optical properties of all the materials deployed in our simulation study were carried out by means of spectroscopic ellipsometry on in-house deposited thin films and reported elsewhere, such as in [31,34].

A 3-D sketch of the simulated structures employing textured oxides and textured c-Si are depicted in Fig. 1. In particular, the structures in Figs. 1(a)-1(d) (textured dielectric) exhibit: (i) front side texturing consisting of TiO_2 pyramids with a period (P_f) of 600 nm and a height (h_f) of 750 nm; (ii) a 2-µm thick flat c-Si slab; (iii) back side texturing formed by larger and shallower pyramids of SiO_2 with period (P_b) of 1200 nm and height (h_b) of 300 nm. Regarding the flat surface models in Figs. 1(a) and 1(c), respectively, is that the TiO_2 has a thickness of 47 nm, based on the $\lambda_{ARC}/4{\cdot}n_{TiO2}(\lambda_{ARC})$ rule, where ARC stands for anti-reflective coating and λ_{ARC} = 500 nm. This is the optimal thickness for reducing reflection in the visible portion of the spectrum by inducing destructive interference for the reflected waves. Also essential to know, the SiO_2 layer in Fig. 1(a) is 100-nm thick, the typical value for which plasmonic resonances are completely blue shifted in the UV region, so that absorption in the silicon slab is not hindered [35]. Similar models for textured c-Si cells were also simulated as sketched in Figs. 1(e)-1(h). In this case, front / back texturing consisted of pyramids made of c-Si with the same dimensions as the ones realized in previous cases based on TiO_2 and SiO_2. The structures could be further optimized by using of non-commensurate periodicities [19], but it is not discussed here for brevity, not having a very large effect on final results. All

#257616 Received 18 Jan 2016; revised 26 Feb 2016; accepted 29 Feb 2016; published 17 Mar 2016

textured c-Si slabs have an *equivalent* thickness ($d_{\text{Eq. (-)c-Si}}$) of 2 µm (i.e. slabs' volume is the same as that of a flat c-Si slab having $d_{\text{c-Si}}$ = 2 µm). The front TiO_2 and the back SiO_2 are merely 47-nm thick and 100-nm thick and serve either as flat coatings as in Figs. 1(e)-1(g) or as conformal coatings as in Figs. 1(f)-1(h). Models sketched in Figs. 1(a) and 1(e) were the same and thus simulated only once.

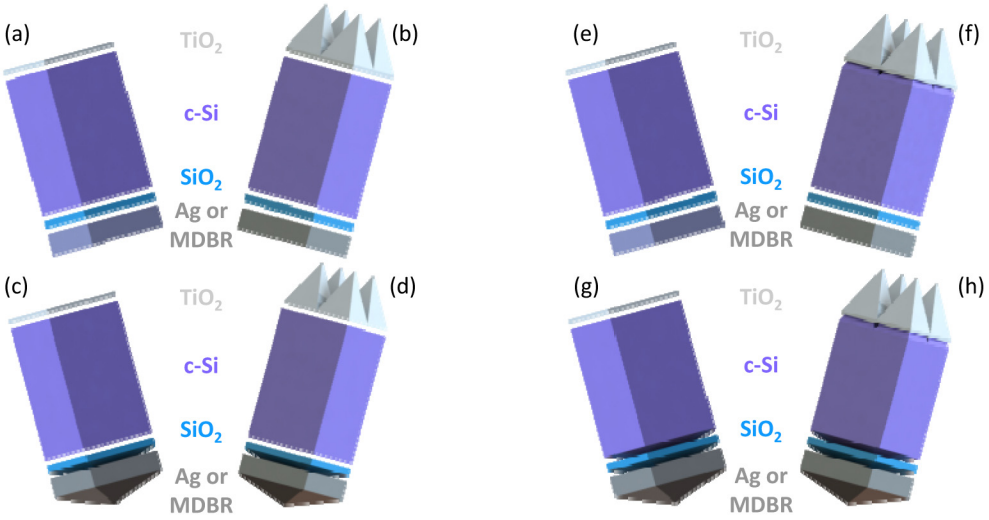

Fig. 1. (a-d) Expanded 3-D rendering of dielectric-textured models used in simulations, indicating materials used: (a) flat reference, (b) structure with texturing only at the front side, (c) structure with texture only at the back side and (d) structure with decoupled front/back texturing. The flat c-Si slabs are 2-µm thick. (e-h) Expanded 3-D rendering of silicon-textured models used in simulations, indicating materials used: (a) flat reference, (b) structure with texturing only at the front side, (c) structure with texture only at the back side and (d) structure with decoupled front/back texturing. The textured c-Si slabs are 2-µm thick *equivalent*. Due to the study of two different back reflectors (Ag and MDBR), the total number of simulated models was 14, since models in (a) and (e) are the same.

As for the absorber thickness, while the ultimate efficiency in c-Si PV technology can be achieved with ~40-µm thick c-Si [36], we chose to focus on 2-µm thick architecture for four main reasons. First, with 1-to-5-µm thick absorber it is possible to observe wave guided modes, which can possibly result in an implied photo-generated current density beyond that predicted by the $4n^2$ limit. That is, we wanted to see whether the front side textured dielectric could trigger some wave guided modes in the flat absorber. Second, a thickness of 2 µm is thin enough to observe wave guided modes but still thick enough to distinguish the optical effect of the front texture from that of the rear texture. Third, 2 µm is a typical thickness of ultra-thin silicon absorbers in modelling studies concerning nc-Si:H, µc-Si:H, poly-Si, mc-Si and c-Si [37]. Fourth, we simulated 50-µm thick c-Si slab with front dielectric textures and rear DBR achieving good light in-coupling but virtually no scattering at all [38], as the absorption in silicon followed the trend of the standard double pass. Especially knowing the last result, we wanted to examine the thickness for which the front dielectric textures could become more effective. Therefore in this study we do not seek to demonstrate the ultimate possible photo-current density in relation to the highest possible conversion efficiency of c-Si solar cells, but rather elaborate on the optical effect that textured dielectrics have on a flat absorbing slab with respect to a textured absorbing slab merely coated with dielectrics.

About the gratings shape, in our previous studies [39] and literature (e.g [40].), it was found that pyramidal structures are - at least - not second from optical point of view to other structures with similar geometrical dimensions and for similar thickness of the absorber material (e.g. rectangular gratings [41], convex gratings [42], concave gratings [43]). For the front side of an absorbing dielectric slab, tapered / pyramidal textures, such as those reported

#257616 Received 18 Jan 2016; revised 26 Feb 2016; accepted 29 Feb 2016; published 17 Mar 2016

in this work, exhibit an optical behaviour very close to an ideal multiple-ARC, for which a very large number of layers would be needed to achieve broad-band light in-coupling. This is due to the smooth matching of the refractive index from the incident medium (in this case air) to the absorber material (in this case silicon). For the rear side, the usage of pyramidal-like textures have been reported in both experimental and modelling studies to have strong impact on the absorption of light in the absorber material [18,20,31,39,44,45]. While we have no absolute evidence that pyramidal texturing is the absolute best for our purposes, we can safely assume that our optical results are not second in performance to those carried out with our same models but endowed with different shapes (rectangular, concave, convex gratings). In this respect the reader can refer to the following Section 2.3. Therefore, since this study focusses on the comparison between a flat absorber against its textured counterpart, we do not lose the generality of our scientific message. In terms of optical performance, the optical outcome of the proposed pyramidal texturing as reported in the following sections could be further improved either by re-arranging the current rectangular 2-D periodic lattice in an hexagonal one [46] or by choosing non-commensurate periodicities [19]. Finally, our previous studies on pure optical system [20] or complete solar cell devices [25] endowed with decoupled front/rear textures or modulated surface textures indicate that the combination of our tapered front nano-texture and micro-scale pyramids results in excellent light in-coupling and long wavelength light scattering in 20-to-280-μm thick wafers. That is, our simulated models with decoupled textures are expected to work well not only in 2-μm thick c-Si slabs but also in thicker slabs. Finally, as for the geometrical parameters of the front texture, as long as the dimensions are in sub-micron scale (100 – 1000 nm) and the aspect ratio is more than one, a flat band light in-coupling can be achieved. Fine tuning of such dimensions may widen the light in-coupling wavelength range.

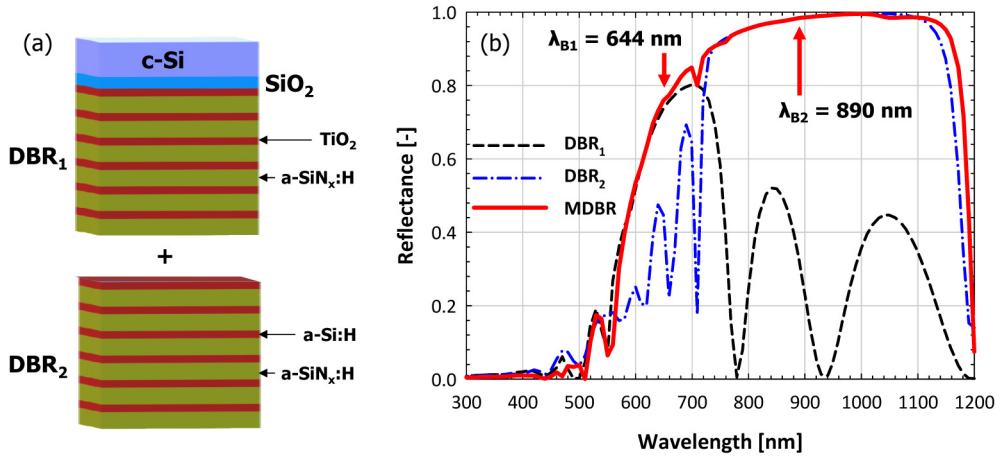

Fig. 2. (a) Structure of the MDBR (dimensions are not to scale) posed at the back side of c-Si slab coated with SiO_2 dielectric spacer layer and (b) reflectance at SiO_2 / MDBR interface inside c-Si bulk.

The choice of dielectric materials such as TiO_2 at the front side and SiO_2 at the rear side was mainly motivated by optical considerations. In fact, TiO_2 is a wide band gap material with relatively high refractive index, helping refractive index matching between air and silicon when structured in a tapered manner at the front side. On the other hand, SiO_2 with its low refractive index determines a high refractive index mismatch between the silicon absorber and the back reflectors. Such mismatch could be in principle surpassed by the refractive index of MgF_2, which is even lower than that of SiO_2; however, SiO_2 has still an edge regarding in-fabrication process compatibility of c-Si solar cells, especially in case of high-thermal budget (> 850 °C) architectures. Moreover, pyramid-textured SiO_2 in the role of periodic grating at

#257616 Received 18 Jan 2016; revised 26 Feb 2016; accepted 29 Feb 2016; published 17 Mar 2016

the rear side also effectively acts as spacer layer in shifting towards short wavelengths plasmonic losses arising at the textured interface with metal [35,47].

For all simulated structures we applied either a 300-nm thick Ag back reflector (Ag BR) or an MDBR. The latter is the result of two different Distributed Bragg Reflectors (DBRs) placed on top of each other as shown in Fig. 2(a). The first DBR (DBR_1) consisted of 6 pairs of hydrogenated amorphous silicon nitride (a-SiN_x:H, 90 nm) and TiO_2 (64 nm) layers. Such reflector is designed to ideally deliver R = 100% in the wavelength range between 580 nm and 723 nm (Bragg wavelength: λ_{B1} = 644 nm). The second DBR (DBR_2) was made of 6 pairs of a-SiN_x:H (125 nm) and hydrogenated amorphous silicon (a-Si:H, 60 nm) layers. DBR_2 is also designed to ideally deliver R = 100% but in the wavelength range between 722 nm and 1159 nm (λ_{B2} = 890 nm). Therefore, as reported in Fig. 2(b), when stacking DBR_1 and DBR_2, a reflectance very close to 100% can be delivered in a broad wavelength range [580 nm, 1159 nm]. At such wavelengths light penetration depth in c-Si becomes larger than the thickness of the absorber layer (2 μm) and therefore high internal rear reflectance is necessary to enhance the length of light's path in the absorber. DBR_2 is located below DBR_1 to reduce parasitic absorptance in a-Si:H layers.

3. Results and discussion

3.1 Flat references

As a start, we simulated the flat model with either Ag BR or MDBR. This test was to verify the goodness of our dielectric MDBR to act as a state-of-the-art metallic reflector. Results show that there is no major difference between the performance of the two back reflectors (see Fig. 3). Both of them give similar values of absorption in silicon and total cell reflectance. So we can conclude that the MDBR on a flat interface not only ensures sufficient reflectivity in the desired wavelength range but also does not let the electromagnetic field propagating through it, resulting in limited T losses at least until ~1150 nm. Consequently, no big difference in the implied photo-generated current density of the absorber is observed (see Fig. 4). For these flat optical systems the reflectance is rather high, due to (i) poor in-coupling of photons at the air / optical system interface and (ii) no trapping of light in the absorber. As it can be seen in following sections, these loss mechanisms can be reduced by texturing only front or back side or both sides, resulting in broad-band quenching of reflectance.

3.2 Front textured structures

Introduction of a nano-texture at the front side of a dielectric slab or of a solar cell allows for a better light in-coupling into the device. This contributes to a reduction of total cell reflection by reducing the reflectivity of the top layer. Previous work carried out in our group [19,20,25] showed that high aspect ratio features characterized by sub-micron geometrical dimensions can accomplish very low values of R. Also for this work it was decided to employ high aspect-ratio pyramids at the front side of our models (P_f = 600 nm, h_f = 750 nm).

Looking at $J_{ph\text{-}Si}$, results show that the MDBR performs slightly better than the Ag BR in both flat c-Si and textured c-Si models ($\Delta J_{ph\text{-}Si}$ = 1.9 mA/cm^2 in case of textured oxides, $\Delta J_{ph\text{-}Si}$ = 1.1 mA/cm^2 in case of textured silicon, see Fig. 5). For both BRs, the structure with textured c-Si can deliver a higher absorption enhancement with respect to the equivalent architecture made of textured TiO_2. The reason for that is related to the decrease of the optical losses at the front side due to a better light in-coupling for textured c-Si structure compared to the flat one. The Si texturing, in fact, provides a smoother grading of the refractive index from air (n_{air} = 1) to bulk c-Si ($n_{c\text{-}Si}$ ~3.5), hence the reflectivity of the top layer is lower.

#257616 Received 18 Jan 2016; revised 26 Feb 2016; accepted 29 Feb 2016; published 17 Mar 2016

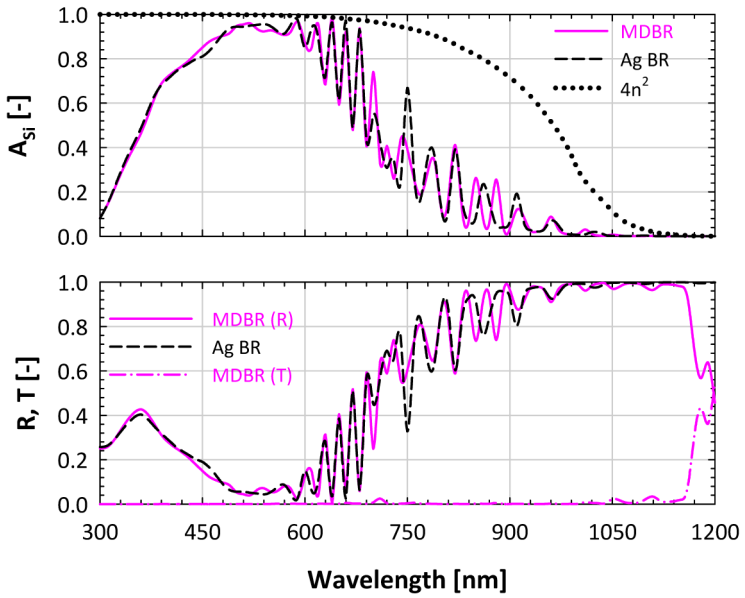

Fig. 3. The absorption, reflectance and transmittance of the flat references with Ag BR (black curves) and MDBR (purple curves). The $4n^2$ curve (black dotted line) represents the Yablonovitch limit for a 2-μm thick c-Si slab.

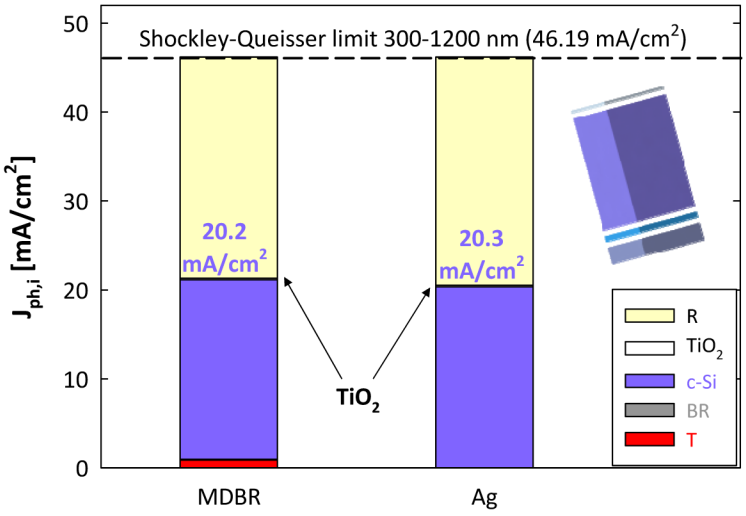

Fig. 4. Implied photo-generated current density of the flat references with MDBR (left side) and Ag BR (right side). The sketch in the inset is Fig. 1(a) or Fig. 1(e).

Nevertheless, the TiO_2 pyramids have good anti-reflective properties, as can be seen in Fig. 6. Here, we compare the simulated absorptance and reflectance of models with TiO_2 pyramids, the flat reference depicted in Fig. 1(a), and an architecture with cylindrical TiO_2-based Mie resonators (P_{Mie} = 600 nm, h_{Mie} = 300 nm [26]). The three models were endowed with the same MDBR. The pyramidal texture shows better light in-coupling, especially in the 300-600 nm wavelength range. Consequently, absorptance for these architectures is higher than in devices with Mie resonators (+ 6.4% higher $J_{ph\text{-}Si}$). However, high cell reflectivity at long wavelengths (900-1100 nm) suggests that no significant trapping of light is taking place. In fact, light reflected at the device back side is not scattered into large angles and can be thus

#257616 Received 18 Jan 2016; revised 26 Feb 2016; accepted 29 Feb 2016; published 17 Mar 2016

easily out-coupled at the front side and escape the optical system. To prevent this and increase the optical performance, the introduction of a micrometer-scale back texture is required.

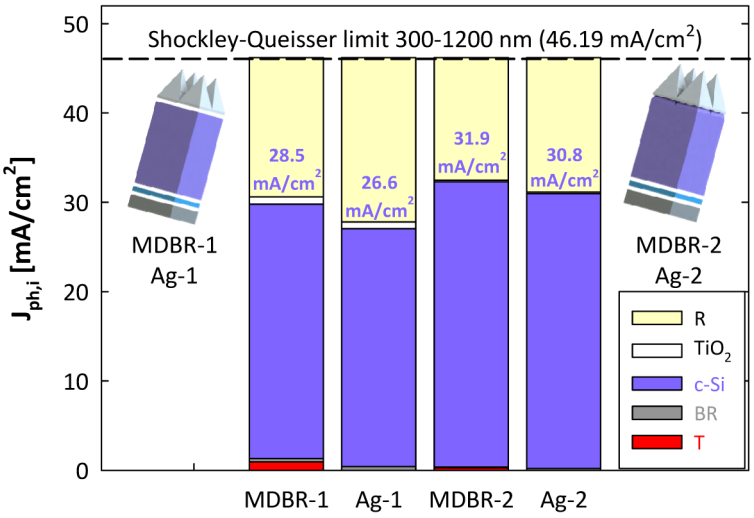

Fig. 5. The absorption, reflectance and transmittance of the front textured structures. MDBR-1 and Ag-1 indicate devices with textured TiO_2, while MDBR-2 and Ag-2 models with textured silicon.

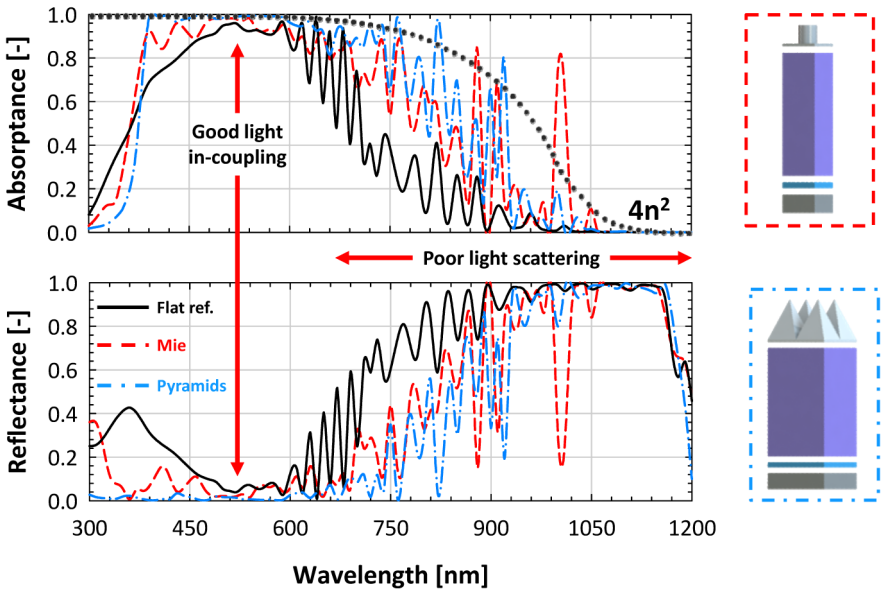

Fig. 6. Absorptance and reflectance of flat reference (black continuous line), architecture with TiO_2-based Mie resonators (red dashed line) and architecture with high aspect-ratio TiO_2 pyramids (blue dash-dotted line).

3.3 Back textured structures

Micron-scale texture at the back side of a solar cell promotes scattering at long wavelengths (λ > 900 nm) [18,20]. Since in this spectral region the absorption of light in c-Si is weak, a light path's enhancement in the absorber can significantly increase the optical performance. Pyramidal structures with relatively large periods can effectively diffract near-infrared light

#257616 Received 18 Jan 2016; revised 26 Feb 2016; accepted 29 Feb 2016; published 17 Mar 2016

into large angles, thus ensuring a substantial lengthening of light's path in the absorber layer. On the other hand, texturing with low aspect-ratio features is desirable for low charge recombination and high electrical performance. For this reason, shallow pyramids were used in this work (P_b = 1200 nm, h_b = 300 nm).

Once again looking at $J_{ph\text{-}Si}$, results show that the Ag BR performs better than the MDBR in both flat c-Si and textured c-Si models ($\Delta J_{ph\text{-}Si}$ = 1.4 mA/cm^2 in case of textured oxides, $\Delta J_{ph\text{-}Si}$ = 0.7 mA/cm^2 in case of textured silicon, see Fig. 7). Since the thicknesses of layers in DBR_1 and DBR_2 are optimized for flat interfaces, when the MDBR is applied to a textured surface it allows more light to go through (T losses also at wavelengths λ < 1150 nm) [34]. As seen previously, pyramids of c-Si result in a higher absorptance than features based on a dielectric material (SiO_2 in this case). This result was expected, since c-Si has a higher refractive index than SiO_2 ($n_{c\text{-}Si}$ ~3.5, n_{SiO2} ~1.5). Thus, more diffraction modes can be excited at the c-Si / SiO_2 / BR interface (c-Si pyramids) than at the SiO_2 / BR interface (SiO_2 pyramids).

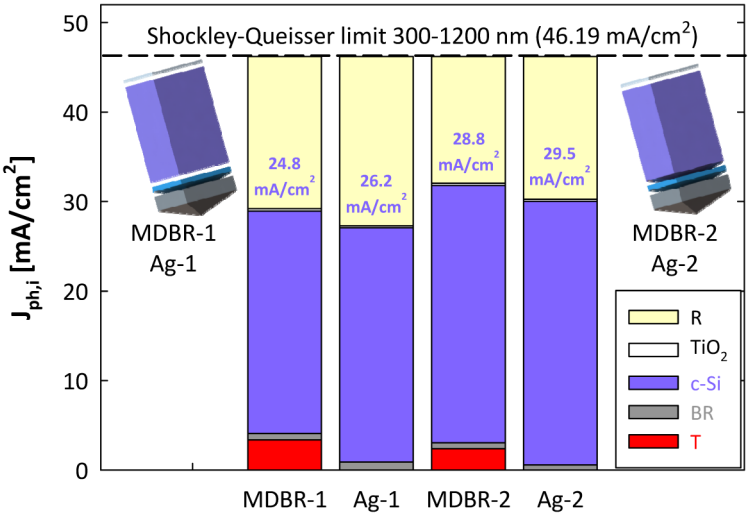

Fig. 7. Architectures with flat front side and back texturing. MDBR-1 and Ag-1 indicate devices with textured SiO_2, while MDBR-2 and Ag-2 models with textured silicon.

3.4 Decoupled front/back texture

Finally we combined nano-scale high-aspect ratio features at the front side for broad-band light in-coupling with micron-scale shallower pyramids at the back side for light scattering.

By evaluating $J_{ph\text{-}Si}$ in this case of decoupled front/back textured structures (see Fig. 8), results show that the MDBR performs better than Ag BR when dielectrics (TiO_2 and SiO_2) are textured ($\Delta J_{ph\text{-}Si}$ = 1 mA/cm^2), while MDBR performs worse than Ag BR in the optical system with textured silicon ($\Delta J_{ph\text{-}Si}$ = –1.9 mA/cm^2). In terms of optical performance, dielectric-coated pyramids based on c-Si are better than textured oxides on flat c-Si, as it was already shown independently for both front- and back-texturing. Considering the same BR, in case of Ag BR (MDBR) the textured dielectrics' model exhibited $\Delta J_{ph\text{-}Si}$ = –7.2 mA/cm^2 (–4.3 mA/cm^2) with respect to the textured c-Si counterpart, equal to a –20.6% (–13%) decrease in optical performance. This difference can be attributed to the textured front TiO_2 at the front side, which absorbs more than the mere TiO_2 coating due to its bigger volume and offers less performant anti-reflective effect with respect to the textured c-Si, and to the textured SiO_2 at the rear side, which develops, for the same periodicity, less diffraction modes with respect to the textured c-Si due to its lower refractive index. Finally, the best textured dielectrics' model, which is fully dielectric, resulted in $J_{ph\text{-}Si}$ = 28.8 mA/cm^2, while the best structure textured c-Si model, which has Ag BR, achieved $J_{ph\text{-}Si}$ = 35.0 mA/cm^2. This is equal to a –17.7% loss in

#257616 Received 18 Jan 2016; revised 26 Feb 2016; accepted 29 Feb 2016; published 17 Mar 2016

optical performance. As it can be seen in Fig. 9, this difference in performance is due to (i) greater absorption losses in the textured front TiO_2 with respect to a 47-nm thick TiO_2 coating the front side of the textured c-Si; (ii) higher transmittance and absorption losses in the MDBR due to its deposition on textured back SiO_2 with respect to the Ag BR deposited on the optimal 100-nm thick SiO_2 coating the back side of the textured c-Si; (iii) narrower light in-coupling and poorer light scattering of the textured dielectrics model with respect to the textured c-Si one.

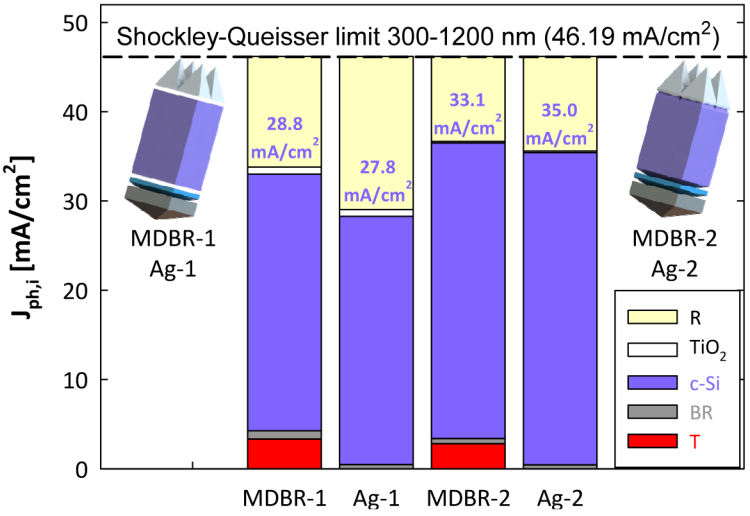

Fig. 8. Architectures with decoupled front/back texturing. MDBR-1 and Ag-1 denote devices with textured dielectrics, while MDBR-2 and Ag-2 models with textured silicon.

4. Conclusions

In this contribution we have modelled ultra-thin *optically-textured* and *electrically-flat* optical systems based on flat c-Si slabs, decoupled front / back dielectric textures and two types of state-of-the-art BRs, Ag and MDBR. The light absorption enhancement of the proposed optical systems was verified with respect to flat reference models and compared to equivalent structures based on textured c-Si merely coated with thin dielectric films at both front and back side and endowed with the same BRs. Our optimized front dielectric textured design on 2-μm thick flat c-Si slab with MDBR resulted in more photo-generated current density in c-Si with respect to the same optical system but featuring state-of-the-art Mie resonators (+ 6.4%), mainly due to an improved light in-coupling between 400 and 700 nm and light scattering between 700 and 1050 nm. On the other hand, using textured dielectric layers resulted in less photo-generated current density in c-Si up to –20.6% with respect to textured c-Si, depending on the type of back reflector taken into account.

Even though the adoption of textured dielectric layers in place of texturing the c-Si absorber means a substantial reduction of implied photo-generated current density, possibly higher V_{OC} and *FF* values can compensate for the reduced optical performance. In fact, in case of properly passivated flat c-Si one can get very low effective surface recombination velocity S_{eff}, but one can nowadays also reach very similar S_{eff} with properly passivated and eventually doped textured c-Si [25,48] without the downside of losing in optical performance. Nevertheless, for devices with textured dielectrics, such as TiO_2 and SiO_2, the simulations show that a configuration with only dielectric supporting layers (MDBR) is better than a structure with a standard Ag BR. Avoiding the use of metal can result in a decrease of manufacturing costs, making this particular device configuration of great interest for ultrathin c-Si solar cells.

#257616 Received 18 Jan 2016; revised 26 Feb 2016; accepted 29 Feb 2016; published 17 Mar 2016

Looking instead at pure performance, devices with decoupled textured c-Si and Ag BR proved to deliver very high implied photo-generated current density with respect to that predict by the $4n^2$ limit calculated for the same height. Actually, as predicted in [23], the $4n^2$ limit was surpassed in several narrow spectral ranges. Such optical performance, united to recent successful efforts in passivating nano- and micro-textured c-Si [25,48] and in growing high-quality ultra-thin c-Si slabs [49], paves the way for the realization of high efficiency ultra-thin c-Si solar cells.

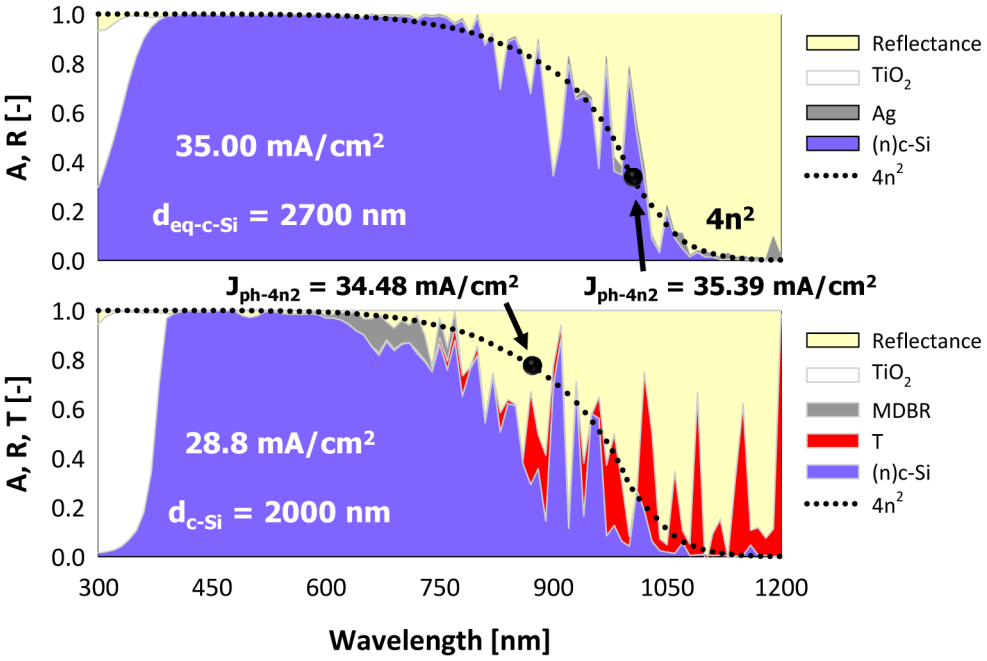

Fig. 9. Absorptance in the c-Si layer and losses (transmittance, reflectance, supporting layers) in optical systems with decoupled front/back texturing. The top panel refers to Fig. 1(h), while the bottom panel refers to Fig. 1(d). For the calculation of the $4n^2$ limit spectra, $d_{Eq.\ (-)c\text{-}Si}$ and $d_{c\text{-}Si}$ indicate the total absorber thickness of textured c-Si and of flat c-Si, respectively.

Acknowledgments

The research leading to these results has received funding from the European Union's Seventh Framework Program FP7/2007-2013 under grant agreement n° 261901 (AGATHA) and from the Dutch Ministry of Economic Affairs under the EOS-LT program (Project No. EOSLT10037). The authors thank dr. S. L. Luxembourg (ECN), dr. P. Spinelli (ECN), dr. M. Verschuuren (Philips) and prof. A. W. Weeber (Delft University of Tecnhology) for useful discussions.

#257616 Received 18 Jan 2016; revised 26 Feb 2016; accepted 29 Feb 2016; published 17 Mar 2016